

1
2 **Localised impacts and economic implications from**
3 **high temperature disruption days under climate**
4 **change**

5 **Authors:**

6 Tim Summers (1), Erik Mackie (2, 3), Risa Ueno (3, 5), Charles Simpson (3, 7), J. Scott
7 Hosking (3, 4), Tudor Suciu (6), Andrew Coburn (1), Emily Shuckburgh (2, 6)

8
9 This paper is a non-peer reviewed preprint submitted to EarthArXiv. It has also been
10 submitted to the journal 'Climate Resilience and Sustainability'.

11 **Affiliations:**

- 12 1. Centre for Risk Studies, Judge Business School, University of Cambridge
13 2. Cambridge Zero, University of Cambridge
14 3. British Antarctic Survey, NERC
15 4. The Alan Turing Institute
16 5. Department of Chemistry, University of Cambridge
17 6. Department of Computer Science & Technology, University of Cambridge
18 7. Institute for Environmental Design and Engineering, University College London
19

20 **Emails:**

21 t.summers@jbs.com.ac.uk
22 erik.mackie@admin.cam.ac.uk
23 risno@bas.ac.uk
24 champs@bas.ac.uk
25 jask@bas.ac.uk
26 ts809@cam.ac.uk
27 andrew.coburn@jbs.cam.ac.uk
28 efs20@cam.ac.uk24
29

30 **Twitter:**

31 @emilyshuckburgh, @Summertim, @ErikMackie, @scotthosking
32

33 **Address for correspondence:**

34
35 Dr T Summers,
36 Centre for Risk Studies,
37 Cambridge Judge Business School,
38 University of Cambridge,
39 Trumpington Street,
40 Cambridge
41 CB2 1AG,

42 UK

43

44 t.summers@jbs.com.ac.uk

45 Tel +44 (0)1223 339700

46

47 Data availability: Our analysis is based on data available via CEDA's data analysis
48 environment JASMIN <https://help.jasmin.ac.uk/article/189-get-started-with-jasmin> .

49 Funding: No directed funding was used for this work.

50 Conflict of interests: The authors are unaware of any conflicts.

51 Ethics approval: The authors follow the core practices of the Committee on Publication
52 Ethics.

53 Reproducible material from other sources: except where noted, material from other sources
54 has not been used.

55 Clinical trials: Not applicable.

56

57 Abstract

58 Most studies into the effects of climate change have headline results in the form of a global
59 change in mean temperature. More useful for businesses and governments however are
60 measures of the localised impact, and also of extremes rather than averages. We have
61 addressed this by examining the change in frequency of exceeding a daily mean
62 temperature threshold, defined as "disruption days", as it is often this exceedance which has
63 the most dramatic impacts on personal or economic behaviour. Our exceedance analysis
64 tackles the resolution of climate change both geographically and temporally, the latter
65 specifically to address the 5-20 year time horizon which can be recognised in business
66 planning.

67 We apply bias correction with quantile mapping to meteorological reanalysis data from
68 ECMWF ERA5 and output from CMIP5 climate model simulations. By determining the daily
69 frequency at which a mean temperature threshold is exceeded in this bias-corrected dataset,
70 we can compare predicted and historic frequencies to estimate the change in the number of
71 disruption days. Furthermore, by combining results from 18 different climate models, we can
72 estimate the likelihood of more extreme events, taking into account model variations. This is
73 useful for worst case scenario planning.

74 Taking the city of Chicago as an example, the expected frequency of years with 40 or more
75 disruption days above the 25°C threshold rises by a factor of four for a time period centred
76 on 2040, compared with a period centred on 2000. Alternately, looking at the change in the
77 number of days at a given likelihood, an example is Shenzhen, where the number of
78 disruption days in a once-per-decade event exceeding the 25°C or 30°C threshold is
79 expected to rise by a factor of four.

80 In a future stage, superimposing these results onto maps of, for instance, GDP sensitivity or
81 production days lost, will provide more accurate and targeted conclusions for future impacts
82 of climate change. This method of quantifying costs on business-relevant timescales will
83 enable businesses and governments properly include risks associated with facilities, plan
84 mitigating actions and make accurate provisions. It can also, for example, inform their
85 disclosure of physical risks under the framework of the Task Force on Climate-related

86 Financial Disclosures. This approach is equally applicable to other weather-related, localised
87 phenomena likely to be impacted by climate change.

88 **Keywords:**

89 economic, disruption, climate, temperature, bias, correction, exceedance

90 **Introduction**

91 Human-induced climate change has resulted in over 1.0°C of global warming to-date, when
92 compared with pre-industrial levels (IPCC 2021). The impacts of this warming trend on
93 human and natural systems are already being felt around the world, in part through an
94 increase in the likelihood of extreme weather events such as heatwaves (Seneviratne et al.
95 2021) (Ciavarella et al. 2021). For example, the recent Siberian heatwave of summer 2020
96 has been shown to be at least 600 times more likely as a result of human-induced climate
97 change(Ciavarella et al. 2021), while the probability of the conditions occurring that led to the
98 2019/2020 Australian bushfires are estimated to have increased by at least 30% since 1900,
99 due to anthropogenic climate change (van Oldenborgh et al. 2020). These risks will increase
100 with future warming.

101 The acute impact of climate change on business and society can be directly observed
102 through changes to the tails of climatic distributions, as extreme events become more likely
103 or more severe. But they are much harder to infer from apparently small changes in central
104 statistics like the rise in the annual global average temperature. Extreme weather events can
105 have adverse financial impacts on businesses through damage to physical assets, disruption
106 or reduction in productivity of operations and supply chains, and impacts to market demand
107 for products and services (Handmer et al. 2012).

108 These risks are of growing concern for businesses, and many corporations are trying to
109 understand how present and future changes in extreme weather risk are likely to affect them.
110 Organisations are under pressure to take action to address environmental, social and
111 corporate governance (ESG) demands, and for strategic and competitive reasons, as well as
112 address regulatory requirements or other liabilities they may face. Mapping the geographical
113 overlap of extreme weather events and business systems is key to providing insight to global
114 corporates of the exposure of their entire value chains to physical climate change risk.

115 These needs are framed by the recommendations of the Task Force for Climate-related
116 Financial Disclosures (TCFD), which has been voluntarily adopted by more than 2,600
117 global organisations as of September 2021, and multiple nations around the world are now
118 introducing legislation for official TCFD-aligned reporting requirements (Quarles 2021).
119 Investors are mobilising to pressure companies to respond to the TCFD recommendations
120 and disclose climate-related risks, with the threat that they will be less inclined to invest in
121 companies that fail to do so (Eccles, R. and Krzus, M. 2018). Companies that comply with
122 the recommendations will have better strategies to adapt to climate change and may be
123 more able to harness any potential opportunities that climate change presents.

124 The TCFD includes a recommendation to describe the impacts of acute (i.e. extreme)
125 weather events, causing physical risks on an organisation over three time horizons, typically
126 below 5 years, five to ten years and beyond ten years. Organisations' energies are typically

127 more focused on short time-frames that they use to conduct operational, financial, strategic,
128 and capital planning (TCFD 2020). However, the currently available data and model
129 projections of future changes in extreme weather risk often do not suit the requirements of
130 businesses. Organisations are struggling to reconcile the long-term projections of the
131 consequences of a warmer planet in several decades' time with changes in the frequency,
132 severity, and geography of extreme weather events that are already having financial impacts
133 on their businesses.

134 Economic productivity is particularly sensitive to extreme heat and associated hazards,
135 which can affect large regions simultaneously to produce widespread impacts and economic
136 loss (García-León et al. 2021; Handmer et al. 2012). These impacts are variable across
137 sectors, and particularly affect those relying on labour-intensive activities such as agriculture,
138 manufacturing, and construction (Zuo et al. 2015; Simpson et al. 2021). Human output is
139 impacted through time loss resulting from the heat-induced health outcomes, or
140 'absenteeism', as well as reductions in work productivity and capacity, termed 'presenteeism'
141 (Xia et al. 2018). Infrastructure, transportation, and energy systems are also vulnerable to
142 extreme heat, and physical damage or service outages can severely disrupt supply chain
143 activities and markets for products and services (Forzieri et al. 2018). Major cities, where
144 economic activity is concentrated, are also subject to an urban heat island effect and so heat
145 waves are typically more extreme, and can result in large death tolls and significant
146 economic loss (Mora et al. 2017).

147 Here we present a geographic resolution of one arc-degree grid squares as a starting point
148 for risk assessment of global business activity, namely supply chains, transportation routes
149 and retail distribution, and to demonstrate a methodology that can be refined and improved.
150 This resolution corresponds to approximately a 110 km square at the equator, and a 110 km
151 by 78 km rectangle at a temperate latitude of 45°.

152 Data and Methods

153 We use climate model outputs from the Coupled Model Intercomparison Project Phase 5
154 (CMIP5) to quantify future changes in extreme temperatures for the period 2020-2059,
155 combined with recent historical data from the European Centre for Medium-Range Weather
156 Forecasts (ECMWF) Re-Analysis (ERA5) for the period 1979-2018 (Hersbach et al. 2020,
157 5).¹ The metric used in this paper is the mean daily temperature. Although daily maximum or
158 minimum temperatures, midday temperatures or other measures might be more appropriate
159 for specific tasks (agricultural yields for instance often depend on minimum as well as
160 maximum temperatures), the mean daily temperature is a good proxy for others and more
161 representative of the overall risk, and thus a good starting point for this generalised study. A
162 subset of 18 of the CMIP5 models is used: details are given in the appendix. For all models,
163 only the RCP4.5 emissions scenarios are used as there is little divergence between the
164 pathways prior to 2060. By the year 2040, the middle of the 2020-2059 period examined in
165 this paper, the RCP4.5 scenario corresponds approximately to a 1.5°C warmer world,
166 compared with pre-industrial temperatures. Information from the historical period is used to

¹ Data was accessed through the Centre for Environmental Data Analysis (CEDA), which makes the data available on JASMIN: <https://help.ceda.ac.uk/article/4465-cmip5-data> ; Copernicus Climate Data Store, available from: <https://cds.climate.copernicus.eu/#/search?text=ERA5&type=dataset>

167 identify systematic biases between the climate model simulations and observational data at
168 a local scale and this is used to produce a transfer function to bias correct future projections.

169 A summary of the five-stage approach used is given below, followed by a more detailed
170 description of each step:

- 171 1. ERA5 and CMIP5 data are firstly interpolated onto a common spatial grid.
- 172 2. For each of the models used, at each location, a bias correction to the raw data is
173 calculated based on the observational data. This defines a transfer function that is
174 then used on model predictions to bias-correct each model's future output.
- 175 3. Using the bias-corrected daily mean temperature predictions with specified
176 temperature thresholds, the annual number of days that the mean daily temperature
177 exceeds a defined threshold (the number of "disruption days") is quantified.
- 178 4. The distribution of the number of disruption days is calculated over a 40-year period
179 for each model at each location.
- 180 5. Combining outputs from all models gives an estimate of the likely number of
181 disruption days, for a given temperature threshold, at each location for a specified
182 time period.

183 Re-gridding

184 ERA5 reanalysis and CMIP5 model outputs are interpolated onto a common spatial grid, a
185 necessity given that different models use different grids. The grid is centred on squares one
186 arc degree wide, between 70°S and 70°N, over land mass. This area is chosen since the
187 majority of economic activity takes place over land mass away from the poles. For coastal
188 locations, the centre of the cell used is the centroid of the land mass, to minimise the
189 influence of the ocean. This results in data being obtained for approximately 18,000
190 geographic locations. While this resolution is high enough for many economic activities, any
191 localised temperature influences (including topographic or urban heat island effect) may be
192 under-represented.

193 Bias correction

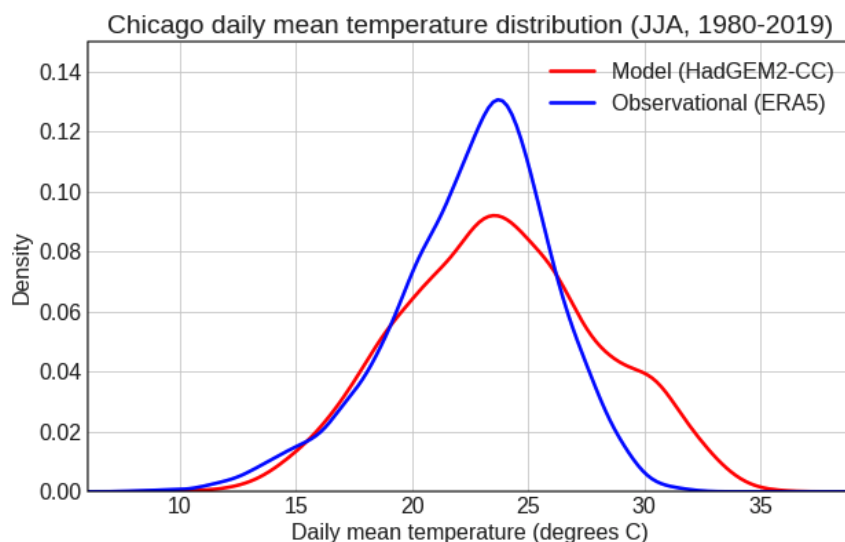
194 Statistical bias correction is a widely adopted post-processing procedure applied to climate
195 model simulation outputs to produce location-specific future projections for impact modelling
196 e.g. (Hawkins et al. 2013). This aims to remove the bias arising from model deficiencies and
197 unresolved physical processes in an individual climate model. The application of bias
198 correction is particularly important when aiming to capture extreme event features in climate
199 model output, as is the focus of this study.

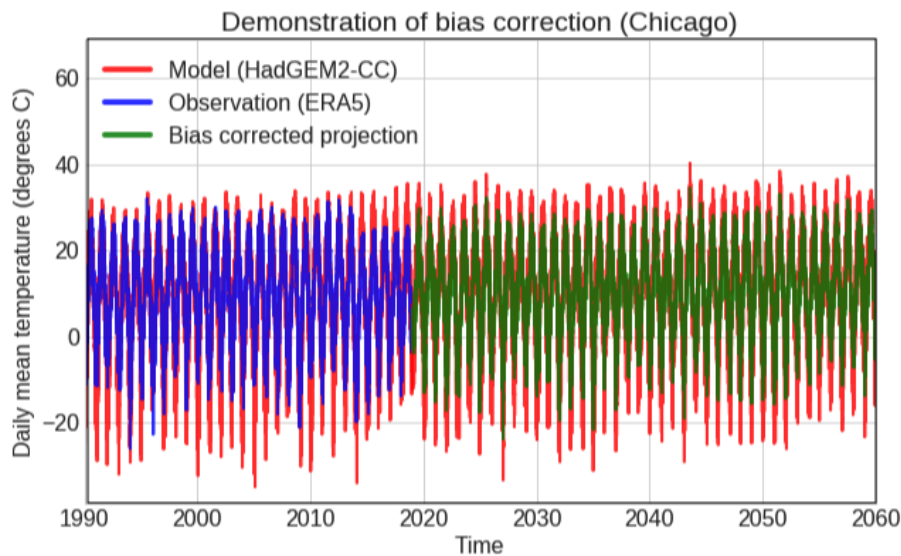
200 One assumption made with this bias-correcting method is that the biases are time-
201 independent. It is possible that global climate systems show high non-linearities in biases,
202 for instance if a 'tipping point' is reached. We hope in the future to improve on the methods
203 described here. Until then, these results should be taken as a best estimate. By including
204 multiple independent models in the analysis, it is believed that this risk is mitigated to a
205 degree. However, it is possible that future measurements could differ markedly from the
206 results described in this paper through inherent uncertainty in our understanding of complex
207 climate systems.

208 In this work, we adopt the quantile mapping method for bias correction, a popular distribution
209 correction technique that has been found to outperform simpler bias correction methods that
210 only account for the mean, or mean and variance of the climate variable (Gudmundsson et
211 al. 2012). Quantile mapping is particularly effective in correcting the tails of a distribution,
212 which is an important consideration in this work concerning extreme events.

213 It has been shown that applying quantile mapping to raw data can artificially alter the trends
214 which can weaken the credibility of the resulting projection, and it has been argued that the
215 climate change signal simulated by the model should be preserved (Haerter et al. 2011;
216 Maraun 2013). Therefore, we detrend the timeseries as a pre-processing step, and
217 subsequently reintroduce the future model trend after applying quantile mapping. This
218 encourages bias correction to account for daily variability without the long-term trend
219 corrupting the overall distribution. We use a 31-day sliding window over the calendar year to
220 avoid climatological discontinuity and use a linear regression to fit a trend for each window in
221 order to capture the long-term signal that may depend on the time of year, as demonstrated
222 in (Hempel et al. 2013). A second order polynomial is used to capture any acceleration in the
223 future climate change signal, which was found to be more robust than a single linear fit (not
224 shown). As with any statistical procedure, bias correction comes with a set of assumptions
225 that are discussed extensively, e.g. (Maraun et al. 2017; Maraun and Widmann 2018).

226 The period 1979 to 2018 inclusive, comprising 40 years of daily data, for which we have
227 overlapping ERA5 measurements and predictions from each CMIP5 model, is used to
228 calibrate the bias correcting transfer function. This is then applied to the future model
229 simulations for the years 2020 to 2059 inclusive to obtain bias-corrected future projections.
230 Transfer functions are derived for each model for every location, a total of approximately
231 330,000. Figure 1 illustrates an example for one location (Chicago) and one model
232 (HadGEM2-CC): the summer daily mean temperature distribution of HadGEM2-CC output
233 and corresponding ERA5 data, illustrating the discrepancy between them (top), and a
234 timeseries of HadGEM2-CC, ERA5 and bias corrected projection (bottom).





236

237 Figure 1: Demonstrating the bias correction: comparison of summer (JJA) daily mean
 238 temperature distributions between raw model output (HadGEM2-CC) and ERA5 in
 239 Chicago (top); demonstration of bias correction as a timeseries of raw model output
 240 (HadGEM2-CC), observational data (ERA5) and bias-corrected output (bottom).

241 Distribution of future temperature disruption days

242 The analysis of the bias corrected data examines the 40-year period 2020 - 2059 and makes
 243 statistical predictions for the number of days with temperatures above a defined threshold in
 244 this period. This is what we refer to as the number of “disruption days”.

245 Counting the number of disruption days in each year during the period gives a distribution of
 246 40 points. This can be visualised as an exceedance plot (i.e. 1 – CDF, the cumulative
 247 distribution function), showing, for a given probability, how many days are expected to be
 248 above a particular temperature. Given that the results have been analysed over a 40-year
 249 period, these results can be interpreted as the best estimate for a period centred on 2040,
 250 the midpoint of the analysis (although there is a long-term trend in temperatures over this
 251 period).

252 Given the relatively low granularity of the output (only 40 data points), kernel density
 253 estimation (KDE) is used to better visualise the underlying statistical process. The KDE
 254 bandwidth used is varied for each location and temperature, and corresponds to 6.7% of the
 255 90% - 10% days: best practice for a Gaussian distribution would be approximately
 256 15%(Silverman, B.W. 1986), but the authors feel that the long tails in this distribution justify a
 257 tighter bandwidth.

258 Results

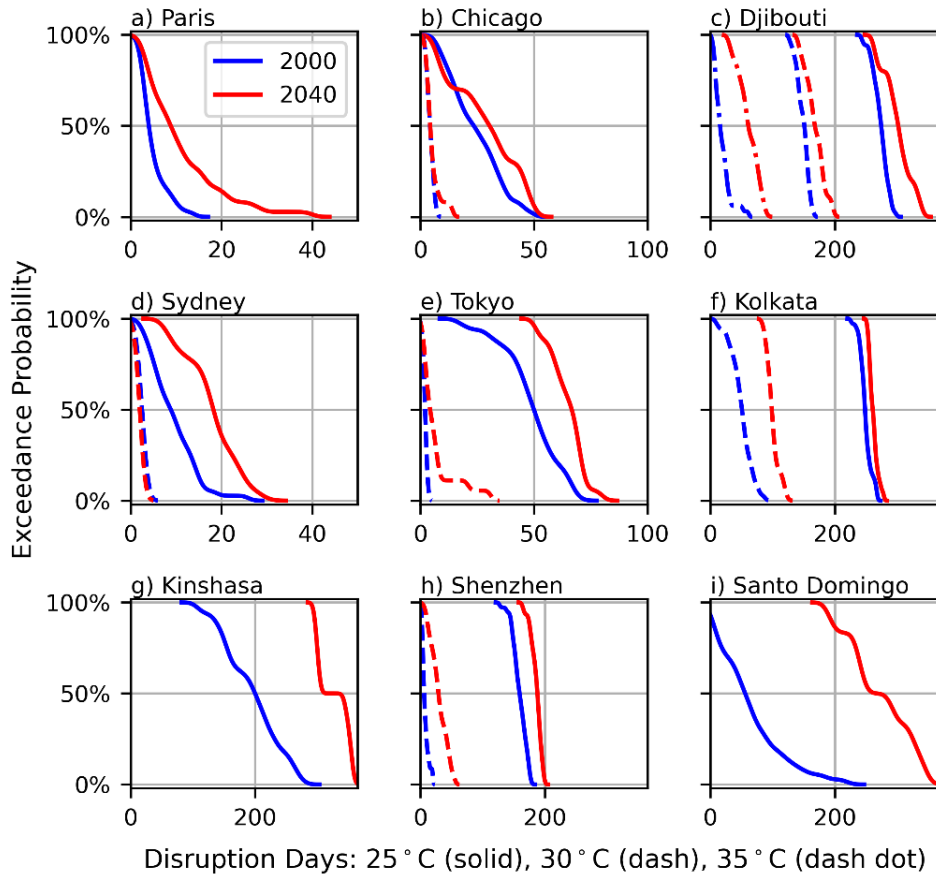
259 Interpretation of a single location

260 Figure 2 shows outputs for a single model (HadGEM2-CC, red line, centred on 2040) for
 261 nine example locations from our global analysis, with up to three temperature thresholds
 262 (25°C, 30°C and 35°C), and compared with the ERA5 historic measurements (blue line,
 263 centred on 2000). The nearest city locations to the actual analysed points are given in Table

264 1. These nine example locations were chosen in order to represent a broad geographic
265 spread of locations across all continents (excluding Antarctica).

266 The disruption days metric is based on specified mean daily temperature thresholds (25°C,
267 30°C and 35°C in this case), and the probability of a threshold being exceeded in any given
268 year. This is shown on the vertical axes in Figure 2: for example, 10% exceedance
269 probability corresponds to a once-per-decade event, or 1% corresponds to a once-per-
270 century event. These thresholds and exceedance probabilities can be adapted according to
271 the business assets in question, to match with the acceptable level of risk to the asset
272 operator, or to reflect the relevant regional context.

273 Figure 2 illustrates that the modelled future changes in the number of disruption days vary
274 widely by geographic location. For example, looking at the example of Paris in Figure 2a, we
275 see an increase of between 10 and 20 disruption days at the 25°C threshold (solid line), for
276 low exceedance probabilities (i.e. 1-in-100 or 1-in-10 year events), but only a small increase
277 of just a few disruption days at higher exceedance probabilities. In contrast, for Santo
278 Domingo in Ecuador (Figure 2i), we see a large increase of over 100 disruption days for the
279 25°C threshold at all exceedance probabilities. Kinshasa in DR Congo (Figure 2g) shows
280 similarly large increases in the number of disruption days at the 25°C threshold. The other
281 locations in Figure 2 also show increases in the number of disruption days at the 30°C
282 threshold (dashed line), and for some (e.g. Kolkata, Figure 2f), the modelled increase at the
283 30°C threshold is greater than at the 25°C threshold. For Djibouti (Figure 2c), we see the
284 greatest increase in number of disruption days at the 35°C threshold (dashed-dotted line).
285 Recall that these thresholds illustrate the mean daily temperature, the peak daily
286 temperature will be significantly higher. The global variation in results is also clear from the
287 global maps shown in Figures 4 & 5.



288

289

290

291

Figure 2: Exceedance plot of number of disruption days above three mean daily temperature thresholds (25°C, 30°C and 35°C), for nine locations, from one model (HadGEM2-CC, red), compared with the historic measurements from ERA5 (blue).

Nearest city	Country	Latitude, longitude
Paris	France	48.5 N, 2.5 E
Chicago	USA	41.5 N, 87.5 W
Djibouti	Djibouti	11.5 N, 42.5 E
Sydney	Australia	33.4 S, 151.25 E
Tokyo	Japan	35.5 N, 139.5 E
Kolkata	India	22.5 N, 88.5 E
Kinshasa	D R Congo	4.5 S, 15.5 E
Shenzhen	P R China	22.74 N, 114.42 E
Santo Domingo	Ecuador	0.5 S, 79.5 W

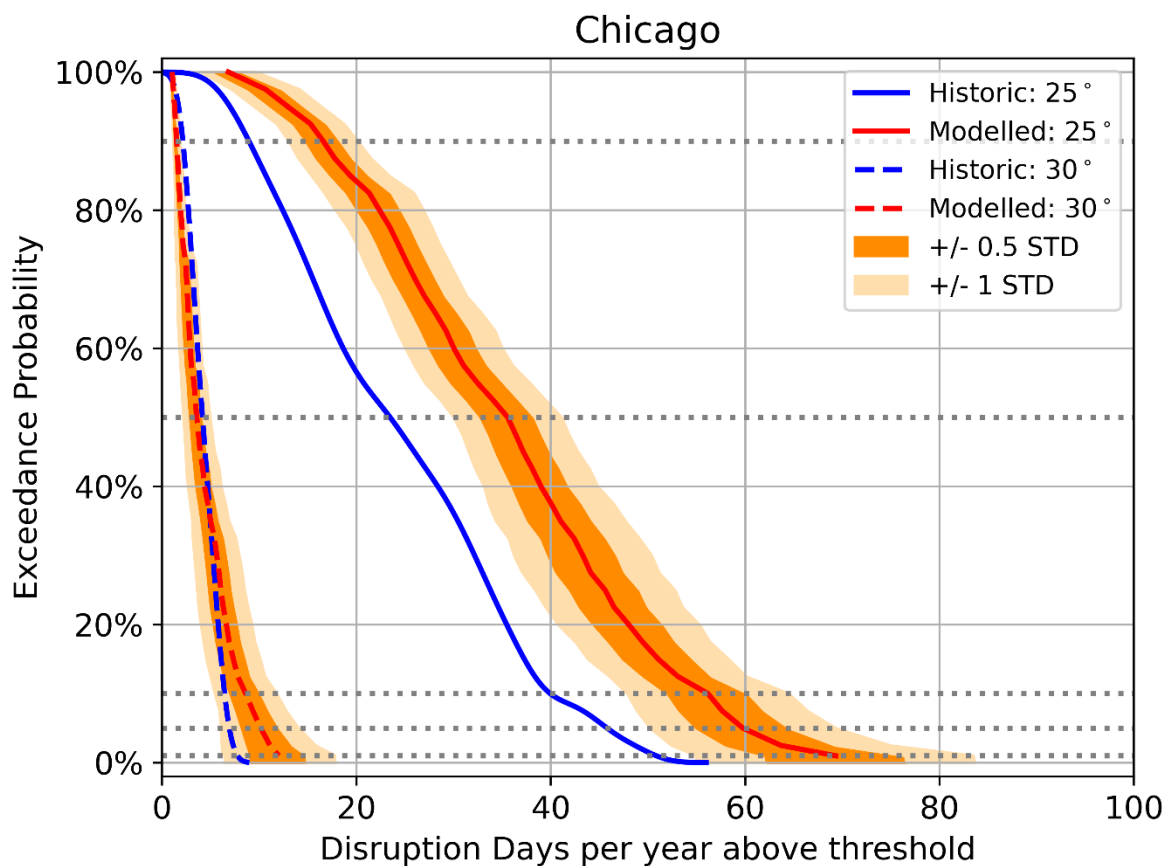
292

293

Table 1: Nearest cities and the exact locations used in the analysis

294 Combining results from all models

295 Each of the 18 models used provides a set of results for each of the approx. 18,000
296 locations. We combine the output from the ensemble of all models to give distributions over
297 the models at each exceedance probability for each temperature threshold. The ensemble-
298 mean provides a “best guess” estimate of the number of disruption days at a particular
299 exceedance probability, while adding a number of standard deviations from the mean
300 provides an indication of a worst-case with a known degree of confidence. Figure 3 shows
301 an example for a single location, the grid cell containing Chicago. The distribution of results
302 between models allows us to give a measure of the assessed likely range (+/- S std) of the
303 prediction around model risk. Statements can be made in the format: ‘At location L, in the
304 period centred on 2040, it is expected that one in N years will have D days disruption at a
305 mean daily temperature above T, with S std of confidence’.



306
307

308 Figure 3: Exceedance plot of number of disruption days above two mean daily
309 temperature thresholds, for one location, with example exceedance probabilities of
310 1%, 5%, 10%, 50% and 90% (grey dotted lines). The ensemble results from all 18
311 bias-corrected models are combined to give statistical measures.

312 For example, referring to the results for Chicago given in Figure 3, we might be interested in
313 a 1-in-10-year scenario, i.e., an exceedance probability, shown on the vertical axis, of 10%.
314 The measurements show that historically there have been approximately 40 days per year,
315 shown on the horizontal axis, where the mean daily temperature has exceeded 25°C (solid
316 blue line): but with the impact of climate change, this is expected to rise to approximately 55

317 days (solid red line). Therefore, we can say: 'In Chicago for the period centred on 2040, we
318 expect every decade there will be one year where 55 days have a mean daily temperature
319 above 25°C, up from 40 days for the period centred on 2000'. The uncertainty between
320 different models can be accounted for by the addition of the following statement: 'there is a
321 16% chance that every decade one year will have 64 days exceeding this threshold'
322 (corresponding to +1 std). This is essential for planning worst case scenarios and takes
323 account of model risk by incorporating an ensemble of results from different groups.

324 Although the change in absolute number of days may be quite small (55 disruption days
325 rather than 40), in a location which is historically ill-prepared for high temperatures, each day
326 can cause a significant cost and an increase in the fraction of days lost could be very
327 significant. One example might be locations in temperate regions that generally do not have
328 air conditioning, where the investment needed to install widespread building cooling capacity
329 would be very significant.

330 Another interpretation is to find the change in frequency for a given number of disruption
331 days. Referring again to Figure 3, there is approximately 10% probability (i.e. 1-in-10 year
332 expectation) of 40 disruption days with a mean daily temperature above 25°C at the baseline
333 2000 condition. Under climate change, for the period centred on 2040 the same number of
334 disruption days is expected with about 38% likelihood, approximately 4-in-10 years. Thus,
335 we can expect approximately four times the number of years with this number of disruption
336 days.

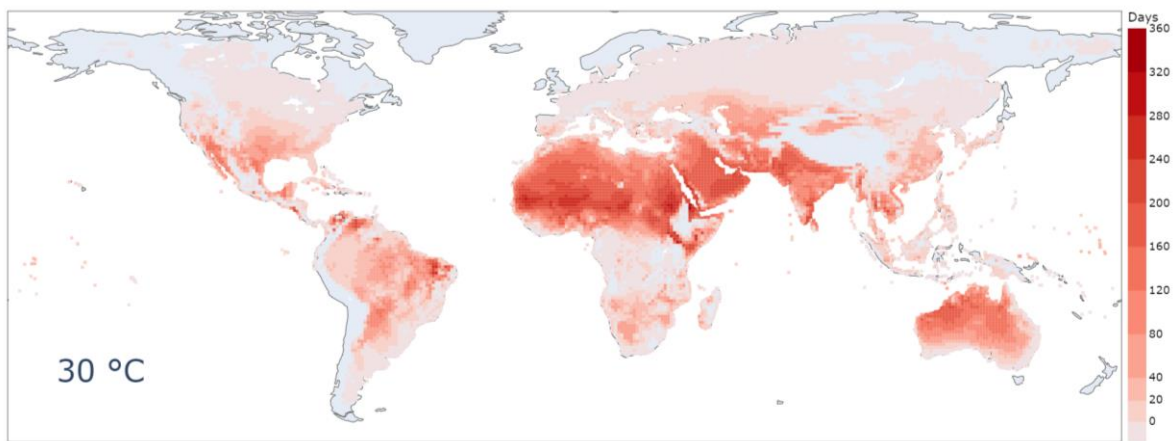
337 This is often a more impactful way to understand the predictions. Risk and operation
338 managers and senior executives might be tempted to regard a 1-in-10 year expected loss as
339 simply a 'risk of doing business' which will generally be smoothed over with preceding and
340 following 'normal' years. If, however this loss approaches a 1-in-2 frequency, it will need to
341 be addressed, mitigated or provisioned. We believe that this method of presenting the
342 impacts of climate change is likely to promote meaningful change from operators and
343 owners of economic assets.

344 Global depiction of results

345 The examples above demonstrate the presented methodology for individual cities, with a
346 moderate temperature threshold. However, this technique is intended for a global application
347 to enable risk analysis of the exposures of global activities and value chains: the example of
348 Chicago above is also applicable to any global location. It is acknowledged that the use of an
349 absolute temperature threshold (e.g. 30°C) has been criticised for not taking into account
350 climate variability (Zuo et al. 2015). However, we suggest that the application of critical
351 thresholds of disruption in this way is a useful method to assess global exposures in a
352 systematic way. Differences in the coping capacity of a specific region or locale to extreme
353 heat can be accounted for through variation of the vulnerability component of a risk
354 calculation.

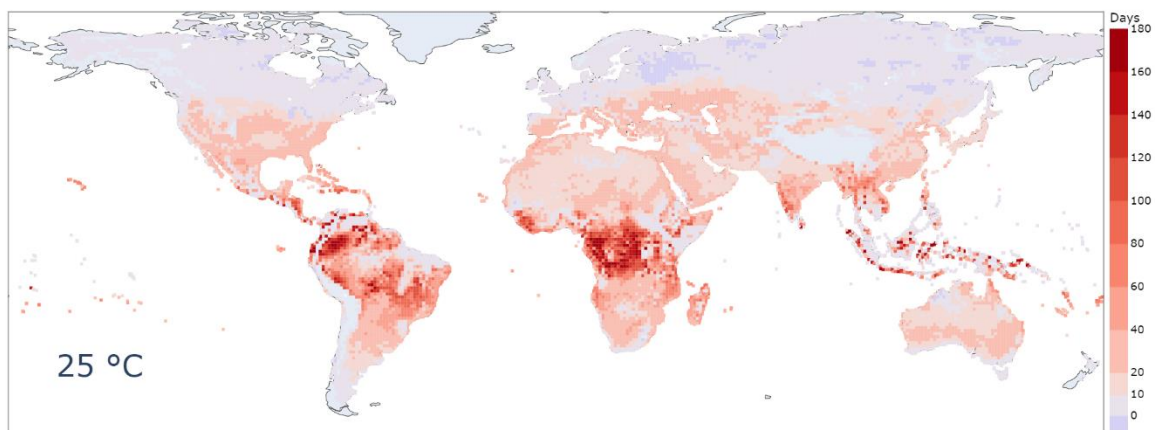
355 Figure 4 shows a global map of the absolute number of disruption days over the 30°C
356 threshold for the 2020-2059 period, at a 10% exceedance probability (one year in 10). For
357 each global location, the mean exceedance from all 18 of the bias corrected models is used.
358 It is clear from the map that for large parts of Saharan Africa, the Middle East and India, in

359 the period centred on 2040, it is expected that 1-in-10 years will have at least 200 disruption
360 days per year over the 30°C threshold, with some regions experiencing up to 360 disruption
361 days per year. A large number of disruption days is also expected in Australia. Some parts of
362 South America, in particular in the Amazon Basin, also show a large number of disruption
363 days. In other regions, including Europe, Sub-Saharan Africa and North America, the
364 absolute number of expected disruption days per year at the 30°C threshold tends to be
365 lower. However, while the absolute number of disruption days may seem low in some
366 regions, the *increase* in the number of disruption days per year may still be higher. This is
367 discussed below.

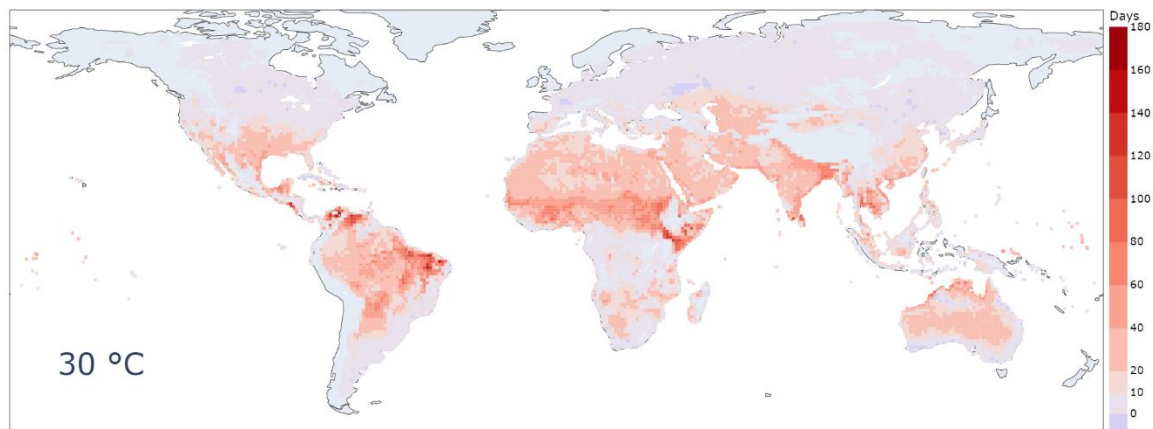


368
369 Figure 4: Absolute number of daily mean disruption days per year over the 30°C temperature
370 threshold for the 2020-2059 period, at a one-year-in-ten exceedance probability.
371

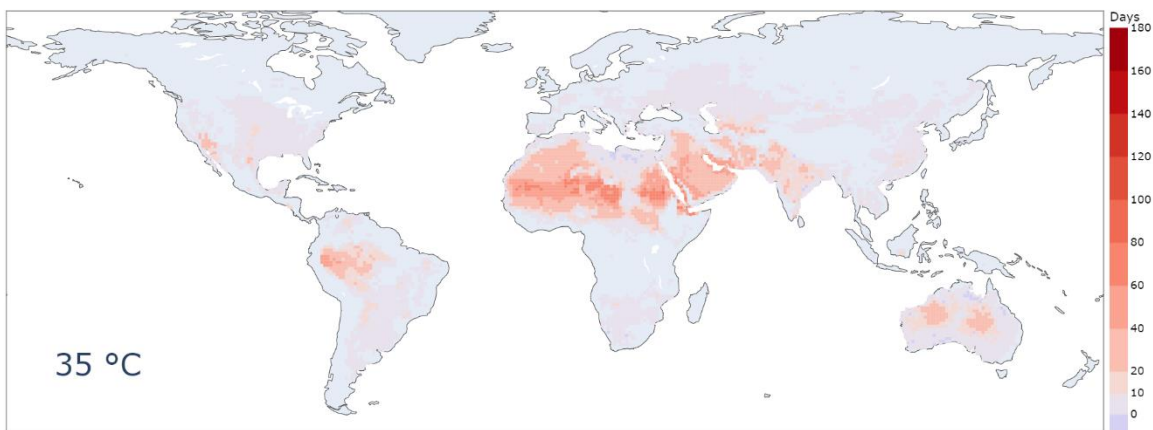
372 Figure 5 shows global maps of the expected increase in the number of disruption days from
373 1979-2018 to 2020-2059, using the threshold of mean daily temperature exceeding 25°C,
374 30°C and 35°C, with a 10% probability of exceedance (i.e. one year each decade).
375 Differences in the impact between regions expected as a result of climate change can easily
376 be seen. For example, Central America and sub-Saharan Africa have a high increase in
377 daily mean 25°C disruption days, but the greatest impact at 35°C is in Saharan Africa and
378 the Middle East, which likely are close to exceeding lower temperature thresholds for most
379 days at historic conditions (illustrated for the example of Djibouti in Figure 2c). This
380 distinction is important, as a temperature threshold that is impactful in one region of the
381 world may be less relevant in another, demonstrating the need for regionally specific
382 thresholds.
383



384



385



386

387 Figure 5: Expected increase in the number of daily mean 25°C (top), 30°C (middle)
 388 and 35°C (bottom) disruption days from 1979-2018 to 2020-2059, at a one-year-in-
 389 ten exceedance probability, mean from all 18 bias-corrected models.

390 Maps such as these can be generated for any temperature or probability threshold,
 391 incorporating if necessary a measure to account for uncertainty between the climate models,
 392 by including a number of standard deviations from the mean between models at each
 393 location, as illustrated for a single location (Chicago) in Figure 3. This approach can be
 394 readily applied to risk assessment in a variety of domains, through analysis of the extreme
 395 heat hazard against exposures and vulnerabilities of specific sectors, such as agriculture
 396 (where agricultural risk models are used to calculate production disruption) or manufacturing
 397 (e.g. to assess rates of absenteeism/presenteeism, reduction of output, energy demands
 398 and air conditioning loads, etc.).

399 Aggregated global results

400 Although the primary focus of this paper is on providing localised estimations of the change
 401 in disruption days, it is also interesting to get a broad measure of the global change in
 402 disruption days. To do so, we divide the globe into three zones by latitude: 0° to 23.5°
 403 ('tropical'), 23.5° to 35.5° ('sub-tropical') and 35.5° to 70° ('temperate'). For each land-mass
 404 grid square in each zone and at each temperature threshold, we calculate the mean of the
 405 baseline number of disruption days and the mean of the increase in disruption days
 406 expected from 1979-2018 to 2020-2059. The results are shown in Table 2.

407

Threshold temp (daily mean)	Zone	Mean baseline number of disruption days for 1979-2018	Mean increase in number of disruption days from 1979-2018 to 2020-2059
25°C	Tropical	237	39
	Sub-tropical	125	20
	Temperate	16	8
30°C	Tropical	51	26
	Sub-tropical	56	20
	Temperate	5	6
35°C	Tropical	17	19
	Sub-tropical	19	12
	Temperate	1.3	4.2

408 Table 2: Mean number of disruption days, and mean increase, for three latitude zones at
409 three temperature thresholds

410 This averaged analysis of course hides a large amount of local data: some localities will
411 have a much larger increase in the number of disruption days and some may have no
412 increase or even a slight decrease (for example some regions of Russia and Canada show a
413 decrease in Figure 5).

414 Given the wide distribution in the increase in the number of disruption days, a more
415 informative way to analyse the data is to ask what fraction of locations in each zone have
416 more than a given number of days increase. We show this fraction in Table 3 for the same
417 temperature thresholds and latitude zones, for 10 and 30 days.

Threshold temp (daily mean)	Zone	Fraction of locations with more than 10 disruption days increase	Fraction of locations with more than 30 disruption days increase
25°C	Tropical	77%	44%
	Sub-tropical	82%	12%
	Temperate	20%	1%
30°C	Tropical	64%	28%
	Sub-tropical	66%	16%
	Temperate	7%	0%
35°C	Tropical	24%	12%
	Sub-tropical	29%	7%
	Temperate	1%	0%

418 Table 3: Fractional increase in the number of locations predicted to have 10 and 30
419 additional disruption days, for three latitude zones at three temperature thresholds

420 Tropical regions are impacted the most with highest fraction of locations suffering 30
421 additional days. For 10 days, sub-tropical regions are approximately equally affected, with
422 temperate latitudes the least impacted. It is worth remembering though that temperate
423 regions may have the biggest financial sensitivity to the disruption days, since many
424 locations will be relatively poorly prepared.

425

426 Discussion

427 Although in some cases the absolute increase in the number of disruption days in the results
428 discussed above is relatively small, we must remember that:

- 429 • This analysis is performed on daily mean temperatures, so a daily peak temperature
430 will be significantly higher
- 431 • Economic processes slow down very rapidly with rising temperature, so (for instance)
432 the prospect of a threefold increase in the number of economically unproductive days
433 would be highly impactful
- 434 • The strong variation between locations (illustrated in Figures 2 & 5) shows that this
435 mean increase includes many locations with a much higher increase
- 436 • Some locations will be less prepared than others. For example, housing and
437 workspaces in many temperate locations do not have air cooling. As a result, an
438 increase in the number of days at even a low temperature threshold could have a
439 higher economic impact than at a sub-tropical location, where at least there is a
440 higher level of preparedness to hot days.

441 Localised Economic Impacts

442 Extreme climate events are known to cause devastating damage, both in human lives and in
443 financial assets. The future 'climate value at risk' of global financial assets is US\$2.5 trillion
444 in the 'business-as-usual' scenario, while the 99th percentile of the possible outcomes gives
445 the value of approximately US\$24.2 trillion (Dietz, Simon et al. 2016). In addition, climate-
446 economic models show that losses from climate change may reach 23% of the global gross
447 product by the end of the 2100 (Patrycja et al. 2021; Burke, Hsiang, and Miguel 2015). Since
448 1970, estimates show that weather-related natural disasters alone caused losses of around
449 US\$1.2 trillion and claimed approximately 1.6 million lives (Swiss Re 2021).

450 Heatwaves have shown increasing trends in frequency, duration and cumulative heat since
451 the mid-twentieth century, and have also shown signs of acceleration of those trends in the
452 presence of global warming (Perkins-Kirkpatrick and Lewis 2020). Those upward trends can
453 be seen in the recent past of such events - the major European heat waves of 2003 and
454 2019 were just 16 years apart but were estimated to be 1-in-450 years and 1-in-283 years
455 events respectively (Munich Re 2004; Ma et al. 2020). Those types of events can be
456 catastrophic for people, countries and businesses, especially if mitigation plans are not in
457 place. The 2003 European heat wave claimed an estimated 35,000 lives, 14,947 out of
458 those in France alone, a country without a strategy against heat waves at the time (Larsen,
459 Janet 2003; Poumadere et al. 2006). Estimates of the financial cost for this event alone are
460 around US\$13 billion, mostly in agricultural costs, which is believed to be a conservative
461 estimate as crops were not usually insured in Europe in 2003 (Munich Re 2004; de Bono et
462 al. 2004).

463 Providing economic loss calculations due to future heat waves is outside the scope of this
464 paper, but the methods and results showcased in this study can provide a good baseline for
465 such estimations. For example, making an assumption that the 1995 Chicago heat wave
466 was a 1-in-100 years event (Karl and Knight 1997) and the fact that this event is part of the
467 1979-2018 timeseries, one can use our disruption days framework to estimate the probability

468 of a similar event arising in the 2040-centered period. Reading from Figure 3, in terms of the
469 same number of disruption days (both 25°C and 30°C thresholds), the probability of having a
470 similar event would increase to 10% (or 1-in-10 years). This result is limited by the
471 aforementioned assumption, but also by the assumption that the ‘disruption days per year’
472 metric is perfectly correlated with the emergence of heat waves. The lack of higher precision
473 in distributions of this metric can also have an effect on this result as the smallest increment
474 in our exceedance probability plots is 2.5%, while the event is assumed to have a probability
475 of 1%. However, this result does show the potential of this type of analysis for the mitigation
476 of future extreme weather events.

477 By knowing the sensitivity to temperatures and the geographic distribution of their
478 operations, it would be feasible for an organization to quantify their expected total financial
479 loss due to temperature disruption days. This could be essential for provisioning, insurance
480 or risk reporting, including TCFD disclosures. It also lays the foundations for planning
481 strategic responses to physical climate change risk.

482 Finally we must remember that the global economy can be highly concentrated on small
483 regions. In an economic ecosystem with small amounts of ‘slack’ in supply chains, a minor
484 disruption to one part can be highly magnified in its overall impact. In this context, even a
485 relatively small change in the number of disruption days at a systemically important location
486 could impact well beyond the affected area. One example of these is logistics hubs: a major
487 disruption at an international port could have long-term, global impacts. This consequence of
488 fragile supply chains underlines further the importance of matching the research described
489 here with comprehensive economic model.

490 Future Work

491 The procedures described in this paper give the first stage of assessing a financial cost at a
492 relatively local resolution from extreme temperature effects, expressed as “disruption days”.
493 However, it needs to be followed by assessments at a local level of economic vulnerability to
494 disruption days. These could be as simple as “the airport will close if the mean daily
495 temperature is above 35°C” or “the cost of electricity generation for the region rises by
496 US\$50 million for each day above 30°C”. At the other extreme, a complex, multi-location
497 operation could assess operations at each location, and apply these vulnerabilities to the
498 disruption days calculated here to give a total expected additional cost. By combining all
499 significant economic activity in a region and estimating vulnerability to extreme weather, it
500 would be possible for a local or national government to estimate the gross effect of
501 temperature disruption days on their economy. A multinational company with economically
502 productive assets spread over many locations could do the same.

503 The general approach used in this study (re-gridding at relatively fine spatial granularity, bias
504 correction of individual models, calculation of the disruption days for each model at each
505 location, followed by ensemble averaging over models to get model risk statistics) can
506 equally well be applied to other extreme weather features which are likely to be affected by
507 climate change, and could be the subject of future work:

- 508
- 509 ● Precipitation. Droughts and flooding have profound effects on many natural and
510 human activities, not least agriculture

- 511 • Multivariate analysis of compound risks. For example, the impacts of humidity
512 combined with temperature, or drought combined with high temperature
- 513 • Low temperature thresholds. Frost days, for example, can limit economic activity in
514 some temperate regions, where freezing temperatures are relatively rare and
515 preparedness is low
- 516 • Quantifying maximum or minimum daily temperatures, rather than mean daily
517 temperatures, might also be interesting as many activities are more accurately limited
518 by daily extremes rather than mean temperatures.

519

520 The methodological analysis presented in this paper could be improved in future studies as
521 and when new datasets and methods become available. In terms of data preparation and
522 pre-analysis, machine learning methods show great promise in improving existing bias
523 correction techniques, and such new methods could be applied to repeat and improve our
524 analysis presented here. While this study has focussed on the use of model results from the
525 CMIP5 generation of climate models, the newly available generation of CMIP6 models have
526 a higher spatial resolution and would allow for the approach in this paper to be repeated with
527 finer geographic grids.

528 Conclusion

529 Using multi-model, bias-corrected results from CMIP5 climate models we estimate the
530 frequency of daily mean temperatures exceeding certain temperature thresholds on
531 “disruption days”, at given locations for a future period centred on 2040, compared with
532 historical observations from ERA5 centred on 2000. Since it is often the exceedance over a
533 threshold, rather than simply the mean annual temperature, that is the determining factor for
534 economic activity, this approach is expected to be a better indicator on the effect of climate
535 change on human and economic activity.

536 Our results allow for the estimation of the increase in the number of disruption days
537 exceeding a certain temperature threshold for a given location and exceedance probability.
538 For example, in Chicago one can expect that by 2040, every decade there will be one year
539 where 55 days have a mean daily temperature above 25°C, up from 40 days for the period
540 centred on 2000. Another way to read the results is that Chicago can expect a fourfold
541 increase in the number of years with at least 40 disruption days above the 25°C threshold by
542 2040.

543 Globally, our results also show that there is broad variation in the modelled increase in
544 number of disruption days, for different locations, temperature thresholds and exceedance
545 probabilities. Central America and Sub-Saharan Africa show the largest increases in number
546 of disruption days at the 25°C temperature threshold, while the greatest increases in
547 disruption days exceeding 35°C are seen in Saharan Africa and the Middle East.

548 By combining these results with the sensitivities of economic activities to temperature
549 thresholds (not described in this paper), it will become possible to estimate the financial
550 impact of climate change on a wide variety of businesses. Examples are logistics (frequently
551 disrupted by weather extremes), outdoor work (where human productivity rapidly falls with
552 temperature) and agricultural yields (which typically fall once a crop-dependant temperature
553 threshold is passed).

554 By knowing locations and the nature of activities through an organisation, it will be possible
555 to estimate, with a given level of confidence over model risk, the financial impact of climate
556 change related changes in temperature.
557

558 Acknowledgement

559 The authors would like to express gratitude to Professor Daniel Ralph and Mr Oliver
560 Carpenter at The Centre for Risk Studies, University of Cambridge, Judge Business School.
561

562 Appendix

563 The CMIP5 models used are: ACCESS1-3, BNU-ESM, CMCC-CMS, CNRM-CM5, CSIRO-
564 Mk3-6, GFDL-CM3, GFDL-ESM2G, GFDL-ESM2M, HadGEM2-CC, HadGEM2-ES, IPSL-
565 CM5A-LR, IPSL-CM5A-MR, IPSL-CM5B-LR, MPI-ESM-LR, MPI-ESM_MR, NorESM1-M,
566 bcc-csm1-1 and inmcm4. A small number of other models were not included either because
567 they had been superseded by later models from the same research group or because of
568 data incompatibilities.

569

570 References

- 571 Bono, Andrea de, Gregory Giuliani, Stéphane Kluser, and Pascal Peduzzi. 2004. 'Impacts of
572 Summer 2003 Heat Wave in Europe'. *UNEP/DEWA/GRID Eur. Environ. Alert Bull.* 2
573 (January): 1–4.
- 574 Burke, Marshall, Solomon M. Hsiang, and Edward Miguel. 2015. 'Global Non-Linear Effect of
575 Temperature on Economic Production'. *Nature* 527 (7577): 235–39.
576 <https://doi.org/10.1038/nature15725>.
- 577 Ciavarella, Andrew, Daniel Cotterill, Peter Stott, Sarah Kew, Sjoukje Philip, Geert Jan van
578 Oldenborgh, Amalie Skålevåg, et al. 2021. 'Prolonged Siberian Heat of 2020 Almost
579 Impossible without Human Influence'. *Climatic Change* 166 (1): 9.
580 <https://doi.org/10.1007/s10584-021-03052-w>.
- 581 Dietz, Simon, Alex Bowen, Charlie Dixon, and Philip Gradwell. 2016. "Climate Value at Risk"
582 of Global Financial Assets'. *Nature Climate Change* 6 (7): 676–79.
- 583 Eccles, R. and Krzus, M. 2018. 'Why Companies Should Report Financial Risks From
584 Climate Change'. *MIT Sloan Management Review*, no. 59: 1–6.
- 585 Forzieri, Giovanni, Alessandra Bianchi, Filipe Batista e Silva, Mario A. Marin Herrera,
586 Antoine Leblois, Carlo Lavalle, Jeroen C. J. H. Aerts, and Luc Feyen. 2018.
587 'Escalating Impacts of Climate Extremes on Critical Infrastructures in Europe'. *Global*
588 *Environmental Change* 48 (January): 97–107.
589 <https://doi.org/10.1016/j.gloenvcha.2017.11.007>.
- 590 García-León, David, Ana Casanueva, Gabriele Standardi, Annkatrin Burgstall, Andreas D.
591 Flouris, and Lars Nybo. 2021. 'Current and Projected Regional Economic Impacts of
592 Heatwaves in Europe'. *Nature Communications* 12 (1): 5807.
593 <https://doi.org/10.1038/s41467-021-26050-z>.
- 594 Gudmundsson, Lukas, John Bjørnar Bremnes, Jan Haugen, and T. Skaugen. 2012.
595 'Technical Note: Downscaling RCM Precipitation to the Station Scale Using Quantile
596 Mapping – A Comparison of Methods'. *Hydrology and Earth System Sciences*
597 *Discussions* 9 (May): 6185–6201. <https://doi.org/10.5194/hessd-9-6185-2012>.
- 598 Haerter, J. O., S. Hagemann, C. Moseley, and C. Piani. 2011. 'Climate Model Bias
599 Correction and the Role of Timescales'. *Hydrology and Earth System Sciences* 15
600 (3): 1065–79. <https://doi.org/10.5194/hess-15-1065-2011>.

601 Handmer, John, Yasushi Honda, Zbigniew W. Kundzewicz, Nigel Arnell, Gerardo Benito,
602 Jerry Hatfield, Ismail Fadl Mohamed, et al. 2012. 'Changes in Impacts of Climate
603 Extremes: Human Systems and Ecosystems'. In *Managing the Risks of Extreme
604 Events and Disasters to Advance Climate Change Adaptation*, edited by Christopher
605 B. Field, Vicente Barros, Thomas F. Stocker, and Qin Dahe, 231–90. Cambridge:
606 Cambridge University Press. <https://doi.org/10.1017/CBO9781139177245.007>.

607 Hawkins, Ed, Thomas M. Osborne, Chun Kit Ho, and Andrew J. Challinor. 2013. 'Calibration
608 and Bias Correction of Climate Projections for Crop Modelling: An Idealised Case
609 Study over Europe'. *Agricultural and Forest Meteorology*, Agricultural prediction using
610 climate model ensembles, 170 (March): 19–31.
611 <https://doi.org/10.1016/j.agrformet.2012.04.007>.

612 Hempel, Sabrina, Katja Frieler, Lila Warszawski, Jacob Schewe, and Franziska Piontek.
613 2013. 'A Trend-Preserving Bias Correction – The ISI-MIP Approach'. *Earth System
614 Dynamics Discussions* 4 (January): 49. <https://doi.org/10.5194/esdd-4-49-2013>.

615 Hersbach, Hans, Bill Bell, Paul Berrisford, Shoji Hirahara, András Horányi, Joaquín
616 Muñoz-Sabater, Julien Nicolas, et al. 2020. 'The ERA5 Global Reanalysis'. *Quarterly
617 Journal of the Royal Meteorological Society* 146 (730): 1999–2049.
618 <https://doi.org/10.1002/qj.3803>.

619 IPCC. 2021. 'Summary for Policymakers. In: Climate Change 2021: The Physical Science
620 Basis. Contribution of Working Group I to the Sixth Assessment Report of the
621 Intergovernmental Panel on Climate Change'. 2021.
622 <https://www.ipcc.ch/report/ar6/wg1/>.

623 Karl, Thomas R., and Richard W. Knight. 1997. 'The 1995 Chicago Heat Wave: How Likely
624 Is a Recurrence?' *Bulletin of the American Meteorological Society* 78 (6): 1107–20.
625 [https://doi.org/10.1175/1520-0477\(1997\)078<1107:TCHWHL>2.0.CO;2](https://doi.org/10.1175/1520-0477(1997)078<1107:TCHWHL>2.0.CO;2).

626 Larsen, Janet. 2003. 'Plan B Updates - 29: Record Heat Wave in Europe Takes 35,000
627 Lives - Far Greater Losses May Lie Ahead | EPI'. 2003. [http://www.earth-
628 policy.org/plan_b_updates/2003/update29](http://www.earth-policy.org/plan_b_updates/2003/update29).

629 Ma, Feng, Xing Yuan, Yang Jiao, and Peng Ji. 2020. 'Unprecedented Europe Heat in June–
630 July 2019: Risk in the Historical and Future Context'. *Geophysical Research Letters*
631 47 (11): e2020GL087809. <https://doi.org/10.1029/2020GL087809>.

632 Maraun, Douglas. 2013. 'Bias Correction, Quantile Mapping, and Downscaling: Revisiting
633 the Inflation Issue'. *Journal of Climate* 26 (6): 2137–43. [https://doi.org/10.1175/JCLI-
634 D-12-00821.1](https://doi.org/10.1175/JCLI-D-12-00821.1).

635 Maraun, Douglas, Theodore G. Shepherd, Martin Widmann, Giuseppe Zappa, Daniel
636 Walton, José M. Gutiérrez, Stefan Hagemann, et al. 2017. 'Towards Process-
637 Informed Bias Correction of Climate Change Simulations'. *Nature Climate Change* 7
638 (11): 764–73. <https://doi.org/10.1038/nclimate3418>.

639 Maraun, Douglas, and Martin Widmann. 2018. *Statistical Downscaling and Bias Correction
640 for Climate Research*. Cambridge: Cambridge University Press.
641 <https://doi.org/10.1017/9781107588783>.

642 Mora, Camilo, Bénédicte Dousset, Iain R. Caldwell, Farrah E. Powell, Rollan C. Geronimo,
643 Coral R. Bielecki, Chelsie W. W. Counsell, et al. 2017. 'Global Risk of Deadly Heat'.
644 *Nature Climate Change* 7 (7): 501–6. <https://doi.org/10.1038/nclimate3322>.

645 Munich Re. 2004. 'TOPICS Geo 2003'. TOPICS Geo 2003. 2004.
646 [http://www.sfu.ca/geog312/readings/Munich%20Re\(2004\).pdf](http://www.sfu.ca/geog312/readings/Munich%20Re(2004).pdf).

647 Oldenborgh, Geert Jan van, Folmer Krikken, Sophie Lewis, Nicholas J. Leach, Flavio
648 Lehner, Kate R. Saunders, Michiel van Weele, et al. 2020. 'Attribution of the
649 Australian Bushfire Risk to Anthropogenic Climate Change'. *Natural Hazards and
650 Earth System Sciences Discussions*, March, 1–46. [https://doi.org/10.5194/nhess-
651 2020-69](https://doi.org/10.5194/nhess-2020-69).

652 Patrycja, Klusak, Matthew Agarwala, Matt Burke, Moritz Kraemer, and Kamiar Mohaddes.
653 2021. 'Rising Temperatures, Falling Ratings: The Effect of Climate Change on
654 Sovereign Creditworthiness'. 2021.

655 [https://www.bennettinstitute.cam.ac.uk/publications/rising-temperatures-falling-](https://www.bennettinstitute.cam.ac.uk/publications/rising-temperatures-falling-ratings/)
656 [ratings/](https://www.bennettinstitute.cam.ac.uk/publications/rising-temperatures-falling-ratings/).

657 Perkins-Kirkpatrick, S. E., and S. C. Lewis. 2020. 'Increasing Trends in Regional
658 Heatwaves'. *Nature Communications* 11 (1): 3357. [https://doi.org/10.1038/s41467-](https://doi.org/10.1038/s41467-020-16970-7)
659 [020-16970-7](https://doi.org/10.1038/s41467-020-16970-7).

660 Poumadere, Marc, Claire Mays, Sophie Mer, and Russell Blong. 2006. 'The 2003 Heat
661 Wave in France: Dangerous Climate Change Here and Now'. *Risk Analysis: An*
662 *Official Publication of the Society for Risk Analysis* 25 (January): 1483–94.
663 <https://doi.org/10.1111/j.1539-6924.2005.00694.x>.

664 Quarles, R K. 2021. 'Status Report: Task Force on Climate-Related Financial Disclosures'.
665 https://assets.bbhub.io/company/sites/60/2021/07/2021-TCFD-Status_Report.pdf.

666 Seneviratne, Sonia I., Xuebin Zhang, M. Adnan, W. Badi, Claudine Dereczynski, Alejandro
667 Di Luca, S. Ghosh, et al. 2021. 'Weather and Climate Extreme Events in a Changing
668 Climate'. In *Climate Change 2021: The Physical Science Basis. Contribution of*
669 *Working Group I to the Sixth Assessment Report of the Intergovernmental Panel on*
670 *Climate Change*, edited by Valérie Masson-Delmotte, Panmao Zhai, Anna Pirani,
671 Sarah L. Connors, C. Péan, Sophie Berger, Nada Caud, et al. Cambridge University
672 Press.

673 Silverman, B.W. 1986. *Density Estimation for Statistics and Data Analysis*. Chapman &
674 Hall/CRC.

675 Simpson, Charles, J. Scott Hosking, Dann Mitchell, Richard A. Betts, and Emily Shuckburgh.
676 2021. 'Regional Disparities and Seasonal Differences in Climate Risk to Rice
677 Labour'. *Environmental Research Letters* 16 (12): 124004.
678 <https://doi.org/10.1088/1748-9326/ac3288>.

679 Swiss Re. 2021. 'Sigma Explorer'. Sigma Explorer. 2021. <https://www.sigma-explorer.com>.

680 TCFD. 2020. 'Recommendations'. *Task Force on Climate-Related Financial Disclosures*
681 (blog). 2020. <https://www.fsb-tcfd.org/recommendations/>.

682 Xia, Yang, Yuan Li, Dabo Guan, David Mendoza Tinoco, Jiangjiang Xia, Zhongwei Yan, Jun
683 Yang, Qiyong Liu, and Hong Huo. 2018. 'Assessment of the Economic Impacts of
684 Heat Waves: A Case Study of Nanjing, China'. *Journal of Cleaner Production* 171
685 (January): 811–19. <https://doi.org/10.1016/j.jclepro.2017.10.069>.

686 Zuo, Jian, Stephen Pullen, Jasmine Palmer, Helen Bennetts, Nicholas Chileshe, and Tony
687 Ma. 2015. 'Impacts of Heat Waves and Corresponding Measures: A Review'. *Journal*
688 *of Cleaner Production* 92 (April): 1–12. <https://doi.org/10.1016/j.jclepro.2014.12.078>.

689